THE JOURNAL OF BIOLOGICAL CHEMISTRY VOL. 280, NO. 40, pp. 33885–33894, October 7, 2005

Interaction of Hemojuvelin with Neogenin Results in Iron Accumulation in Human Embryonic Kidney 293 Cells*[S]

Received for publication, June 7, 2005, and in revised form, July 28, 2005 Published, JBC Papers in Press, August 15, 2005, DOI 10.1074/jbc.M506207200

An-Sheng Zhang[‡1], Anthony P. West, Jr.[§], Anne E. Wyman[§], Pamela J. Bjorkman[§¶], and Caroline A. Enns[‡]

From the [‡]Department of Cell and Developmental Biology, Oregon Health & Science University, Portland, Oregon 97239, the [§]Division of Biology, California Institute of Technology, Pasadena, California 91125, and the [¶]Howard Hughes Medical Institute, California Institute of Technology, Pasadena, California 91125

Type 2 hereditary hemochromatosis (HH) or juvenile hemochromatosis is an early onset, genetically heterogeneous, autosomal recessive disorder of iron overload. Type 2A HH is caused by mutations in the recently cloned hemojuvelin gene (*HJV*; also called *HFE2*) (Papanikolaou, G., Samuels, M. E., Ludwig, E. H., MacDonald, M. L., Franchini, P. L., Dube, M. P., Andres, L., MacFarlane, J., Sakellaropoulos, N., Politou, M., Nemeth, E., Thompson, J., Risler, J. K., Zaborowska, C., Babakaiff, R., Radomski, C. C., Pape, T. D., Davidas, O., Christakis, J., Brissot, P., Lockitch, G., Ganz, T., Hayden, M. R., and Goldberg, Y. P. (2004) *Nat. Genet.* 36, 77–82), whereas Type 2B HH is caused by mutations in hepcidin. *HJV* is highly expressed in both skeletal muscle and liver. Mutations in *HJV* are implicated in the majority of diagnosed juvenile hemochromatosis patients. In this study, we stably transfected *HJV* cDNA into human embryonic kidney 293 cells and characterized the processing of HJV and its effect on iron homeostasis. Our results indicate that HJV is a glycosylphosphatidylinositol-linked protein and undergoes a partial autocatalytic cleavage during its intracellular processing. HJV co-immunoprecipitated with neogenin, a receptor involved in a variety of cellular signaling processes. It did not interact with the closely related receptor DCC (deleted in Colon Cancer). In addition, the HJV G320V mutant implicated in Type 2A HH did not co-immunoprecipitate with neogenin. Immunoblot analysis of ferritin levels and transferrin-^{55}Fe accumulation studies indicated that the HJV-induced increase in intracellular iron levels in human embryonic kidney 293 cells is dependent on the presence of neogenin in the cells, thus linking these two proteins to intracellular iron homeostasis.

Hereditary hemochromatosis (HH)[2] includes a heterogeneous group of inherited iron overload diseases resulting from mutations in at least the following five genes: *HFE*, hemojuvelin (*HJV*; also called *HFE2*), hepcidin (*HAMP*), transferrin receptor-2, and ferroportin (*FPN*; also called *SLC40A1*) (1, 2). Type 1 HH, the most common form, is caused by mutations of the *HFE* gene and is an late onset, autosomal recessive, low penetrance iron overload disorder (3). Type 2 HH or juvenile hemochromatosis (JH) is a rare autosomal recessive disease with high penetrance that affects young patients of both sexes and that leads to severe clinical complications typically in the first and second decades of life (4, 5). JH results from mutations of either the *HJV* gene (Type 2A) or the hepcidin gene (Type 2B) in early iron loading with similar serum iron parameters and distribution of accumulated iron in organs (2, 6). Both Type 1 HH and JH individuals have increased intestinal absorption and deposition of iron in vital organs, including the liver, heart, and pancreas. However, JH individuals have a higher rate of iron absorption and a more rapid and severe clinical course with a higher frequency of cardiomyopathy, diabetes, and hypogonadism (5).

HJV is a newly cloned gene localized on chromosome 1q21 (6). This region of chromosome 1 was previously linked to JH (7–10). *HJV* has five predicted spliced transcripts encoding three different proteins of 426, 313, and 200 amino acids. Northern blot analysis has indicated high expression in adult and fetal liver, heart, and skeletal muscle with the full-length mRNA as the primary transcript. The encoded protein (HJV) possesses multiple protein domains, including an N-terminal signal peptide, an RGD motif, a partial von Willebrand factor D motif, and a C-terminal transmembrane domain (6). Numerous mutations in *HJV* that cause Type 2A HH have been identified. These include missense, frameshift, and nonsense mutations in either homozygous or compound heterozygous individuals (6, 11–16). Although the amino acid substitution G320V accounts for about two-thirds of Type 2A HH (6), the sporadic distribution of these mutations hints that Type 2A HH is due to the loss of HJV function. Interestingly, the hepcidin levels in these patients are found to be consistently depressed, suggesting that HJV may act as a modulator of hepcidin expression (6). Hepcidin is a small peptide hormone synthesized predominantly in hepatocytes. It is critical for the maintenance of body iron homeostasis through down-regulation of the iron exporter FPN in intestinal endothelial cells and macrophages (17–19). Hepcidin expression is highly regulated by body iron status, hypoxia, and inflammation (20). In contrast, a more recent study found that *HJV* mRNA levels are increased by inflammation, but do not respond to iron status or erythropoietin in mice (21).

HJV shares considerable sequence similarity with the newly identified repulsive guidance molecules (RGMs) (6). In the mouse (m) RGM family, there are at least three members, mRGMa, mRGMb, and mRGMc (22–24). Human HJV is the ortholog of mRGMc (Fig. 1). *In situ* hybridization analysis of the distribution of the various RGMs in mouse embryos has shown that mRGMa and mRGMb are expressed predominantly in distinct, mostly no-overlapping patterns in the developing and adult central nervous systems, whereas mRGMc is expressed mainly in skeletal and heart muscles (22–24). The *in situ* localization of mRGMc is consistent with the Northern blot analysis results of *HJV* mRNA in human tissues and the fact that no neural symptoms have been reported in Type 2A HH patients (6). Functional studies of

* This work was supported by National Institutes of Health Grants DK54488 (to C. A. E.) and R01 DK60770 (to P. J. B.). The costs of publication of this article were defrayed in part by the payment of page charges. This article must therefore be hereby marked "*advertisement*" in accordance with 18 U.S.C. Section 1734 solely to indicate this fact.

[S] The on-line version of this article (available at http://www.jbc.org) contains supplemental figures.

[1] To whom correspondence should be addressed: Dept. of Cell and Developmental Biology, L215, Oregon Health & Science University, 3181 SW Sam Jackson Park Blvd., Portland, OR 97239. Tel.: 503-494-5846; Fax: 503-494-4253; E-mail: zhanga@ohsu.edu.

[2] The abbreviations used are: HH, hereditary hemochromatosis; HJV, hemojuvelin; JH, juvenile hemochromatosis; FPN, ferroportin; RGM, repulsive guidance molecule; m, mouse; DCC, deleted in Colon Cancer; HEK293, human embryonic kidney 293; Tf, transferrin; sHJV, soluble hemojuvelin; TfR, transferrin receptor; PI-PLC, phosphatidylinositol-specific phospholipase C; GAPDH, glyceraldehyde-3-phosphate dehydrogenase; siRNA, small interfering RNA; GPI, glycosylphosphatidylinositol.

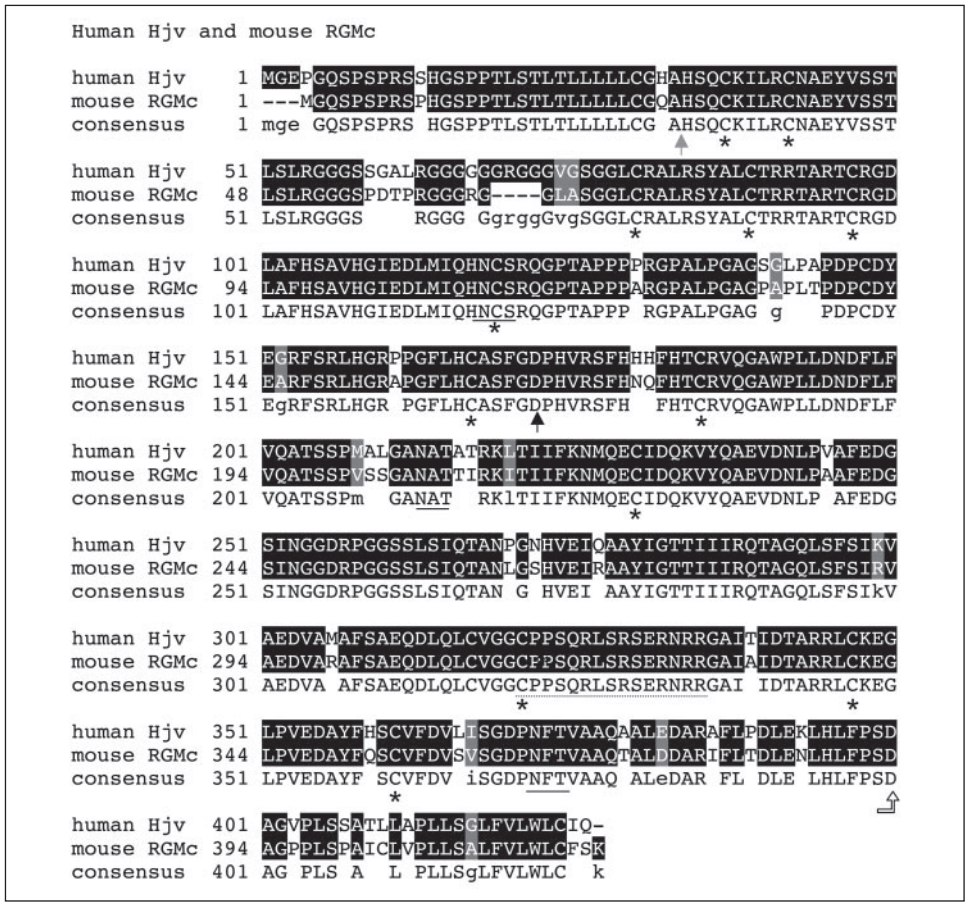

FIGURE 1. **Sequences of human HJV and mRGMc.** Human HJV is 88% identical and 92% similar to mRGMc. Both have a predicted signal peptide cleavage site (*gray arrow*), three consensus sequences for *N*-linked glycosylation (*solid lines*), and 12 Cys residues conserved in HJV and all of the mRGM family proteins (*asterisks*). Both HJV and mRGMc have one predicted acid-sensitive autocatalytic cleavage site (*black arrow*) and a predicted GPI-linked site (*white arrow*). Anti-HJV peptide antibody was generated against the sequence indicated by the *dotted line*.

mRGMa in mouse embryos have revealed that it plays a critical role in the control of cephalic neural tube closure and formation of afferent connections in the dentate gyrus (24, 25). Chicken RGM, an ortholog of mRGMa, has also been reported to be essential for retinotectal map formation in the chick embryo (26). More recent studies have demonstrated that neogenin is the high affinity receptor for chicken and mouse RGMs and that their interaction is critical in the regulation of neuronal survival (27, 28).

Neogenin is a membrane protein. It is closely related to another receptor, DCC (deleted in Colon Cancer), with nearly 50% amino acid identity. Neogenin is widely expressed in different tissues, including muscles and liver (29–31). Functional studies in zebrafish embryos using morpholino oligonucleotides demonstrated that it is essential for neural tube formation and somitogenesis (32), a function similar to mRGMa in mouse embryos (24). This evidence supports the idea that the RGMa/neogenin interaction is indispensable for neural development. On the basis of the high sequence identity of RGMa to RGMc and human HJV, the lack of RGMa in the liver, and finally the presence of HJV and neogenin in the liver (6, 22–24), we speculate that neogenin might also be a candidate receptor for HJV.

In this study, we stably transfected *HJV* cDNA into human embryonic kidney 293 (HEK293) cells and characterized its effect on iron homeostasis. Our results indicate that HJV is processed similarly to other members of the RGM family of proteins. Immunoprecipitation analysis demonstrated that HJV interacts with neogenin, but not with DCC, and that the HJV G320V mutant implicated in Type 2A HH does not bind to neogenin. Immunoblot analysis of ferritin levels and transferrin (Tf)-bound ^{55}Fe accumulation studies showed that the HJV-induced increases in intracellular iron levels in HEK293 cells are dependent on the presence of neogenin in the cells.

EXPERIMENTAL PROCEDURES

Subcloning HJV into pcDNA3—The full-length HJV open reading frame was amplified from a human liver cDNA library by PCR using the Expand high fidelity PCR system (Roche Applied Science) with primers 5′-atgggggagccaggccagtcccctagtcccaggtcctccc-3′ (forward) and 5′-ttactgaatgcaaagccacagaacaaagagcccagaaagga-3′ (reverse). The amplicon was subsequently cloned into the pGEM-T vector (Promega). After the sequence was confirmed by sequencing, the HJV open reading frame was subcloned into the expression vector pcDNA3 (Invitrogen) to make the pcDNA3-HJV construct. To map the fragmentation pattern of HJV, we engineered a modified plasmid by addition of a Myc tag at the position 3 amino acid after the N-terminal signal peptide sequence. To do this, two portions of the HJV open reading frame (the first 111 bp at the 5′-end and the remaining 1170 bp at the 3′-end) were first amplified separately using the primers for the full-length HJV open reading frame cloning (described above) as well as the following primers: 5′-ctcgaggcattgagaatgagcatgtcc-3′ (reverse primer for the former) and 5′-ctcgaggagcagaaactcatctctgaagaggatctgaagatcctccgctgcaatgct-3′ (forward primer for the latter). An XhoI enzyme digestion site was also included in these primers to ligate the two HJV fragments. The PCR amplicons were first cloned into the pGEM-T vector, and their sequences and orientation in the vectors were verified. The 1170-bp 3′-portion of HJV was excised from pGEM-T with XhoI and SphI and subcloned into pGEM-T containing the 111-bp 5′-portion of HJV. The resulting Myc-HJV in pGEM-T (pGEM-T-Myc-HJV) was subcloned into the expres-

sion vector pcDNA3 as follows. Both the pGEM-T-Myc-HJV and pcDNA3 vectors were first linearized by SphI and ApaI digestion, respectively, followed by treatment with the Klenow fragment (New England Biolabs Inc.) to make blunt ends. Myc-HJV was then excised from linearized pGEM-T-Myc-HJV with NotI and ligated with linearized and NotI-digested pcDNA3 to form pcDNA3-Myc-HJV. The construct was verified by sequencing.

The HJV G320V mutant was made using the QuikChange™ XL site-directed mutagenesis kit (Stratagene) following the manufacturer's instructions. The pcDNA3-HJV construct was used as a template. The primers used to introduce the mutation were 5′-gctctgtgttggggtgtgccctccaagtc-3′ (forward) and 5′-gacttggagggcacaccccaacacagagc-3′ (reverse). The G320V mutation in the resulting construct was confirmed by DNA sequencing. No other sequence changes were detected.

The full-length human neogenin cDNA in pcDNA3 was kindly provided by Dr. Eric R. Fearon (University of Michigan Medical School, Ann Arbor, MI). The sequence has been published previously (30).

Transfection—HEK293 cells were cultured in Dulbecco's modified Eagle's medium supplemented with 10% fetal bovine serum and 1 mM pyruvate. All transfections were performed using Lipofectamine reagent (Invitrogen) according to the manufacturer's instruction. Transiently transfected cells were used in experiments ~48 h post-transfection. For stable transfection, transfected cells were selected under 800 μg/ml G418. Positive clones were screened by Western blot analysis. HEK293 cells stably transfected with Myc-HJV, HJV G320V, and empty vector (pcDNA3) were designated Myc-HJV HEK293 cells, HJV G320V HEK293 cells, and control HEK293 cells, respectively. HT29 cells stably transfected either with DCC (HT29-DCC11) or with empty vector (HT29-neo) (33) were kindly provided by Dr. Anna Velcich (Montefiore-Einstein Cancer Center, New York).

Generation of Soluble HJV (sHJV) and Anti-HJV Antibody—A construct encoding a soluble portion of HJV (residues 1–401 inclusive of the HJV signal sequence) with a C-terminal His tag was subcloned into the baculovirus transfer vector pVL1393 (Pharmingen). sHJV was purified from the supernatants of baculovirus-infected High5 cells and buffer-exchanged to 10 mM Tris (pH 8) and 200 mM NaCl, followed by nickel-nitrilotriacetic acid Superflow chromatography (Qiagen Inc.). Protein from an imidazole elution was further purified by gel filtration chromatography in 20 mM Tris (pH 8) and 300 mM NaCl at 4 °C (34). sHJV was used as an antigen to generate polyclonal antiserum in rabbits (Pocono Rabbit Farm & Laboratory, Inc., Canadensis, PA).

Fluorescence Microscopy Analysis—Two days prior to immunofluorescence analysis, Myc-HJV HEK293, HJV G320V HEK293 and control HEK293 cells were seeded onto poly-L-lysine-coated coverslips. After washing with phosphate-buffered saline, cells were fixed with 4% paraformaldehyde in phosphate-buffered saline for 15 min at room temperature. The cells were either blocked directly in 10% fetal bovine serum in phosphate-buffered saline for 1 h at room temperature (nonpermeabilized cells) or treated with 0.2% Triton X-100 in phosphate-buffered saline for 10 min, followed by blocking (permeabilized cells). The cells were then incubated either with affinity-purified anti-Myc monoclonal antibody (for Myc-HJV; a kind gift from Dr. Jan Christian, Oregon Health & Science University) at 1:20 dilution or with rabbit anti-HJV serum (for HJV G320V) at 1:400 dilution for 1 h at room temperature, followed by incubation with either Alexa 594-labeled donkey anti-mouse (1:500 dilution) or goat anti-rabbit (1:500 dilution) antibody (Molecular Probes, Inc., Eugene, OR) as the corresponding secondary antibody. Cells were mounted with ProLong antifade reagent (Molecular Probes, Inc.) and imaged using a Nikon fluorescence microscope (×60 oil immersion lens; Meridian Instrument Company, Inc., Kent, WA).

Immunodetection on Western Blots—Cell lysates from HEK293 and HT29 cells were prepared as described previously (35). Briefly, samples were subjected to 8 or 12% SDS-PAGE under reducing or nonreducing conditions as indicated below. After transferring onto nitrocellulose membrane and blocking with 5% nonfat milk in buffer containing 0.1 M Tris-HCl, 0.15 M NaCl (pH 7.4), and 0.05% Tween 20, immunoblot analysis was performed using mouse anti-Myc monoclonal antibody (1:500 dilution), rabbit anti-HJV peptide antibody (1:1000 dilution; a kind gift from Dr. Silvia Arber, University of Basel, Basel, Switzerland) (24), rabbit anti-HJV serum (1:10,000 dilution), sheep anti-human ferritin antibody (1:1000 dilution; The Binding Site, Ltd., Birmingham, UK), rabbit anti-neogenin antibody H-175 (1:1000 dilution; Santa Cruz Biotechnology, Inc.), mouse anti-DCC monoclonal antibody (1:100 dilution; Oncogene Research Products), sheep anti-transferrin receptor (TfR) antibody (1:10,000), or mouse anti-β-actin monoclonal antibody (clone AC-15, 1:10,000 dilution; Sigma). Blots were visualized by incubation with the appropriate horseradish peroxidase-conjugated secondary antibody and chemiluminescence (SuperSignal, Pierce). Equal protein loading in each lane was verified by both Ponceau S staining and Western blotting for β-actin.

Neutralization of pH in the HJV-processing Compartments—Myc-HJV HEK293 cells (clones 6 and 15) and control HEK293 cells were incubated overnight in the presence or absence of 25 mM NH_4Cl. Cell lysates were prepared as described above and subjected to 12% SDS-PAGE. HJV was detected using anti-HJV peptide antibody at 1:1000 dilution.

Phosphatidylinositol-specific Phospholipase C (PI-PLC) Cleavage of Cell-surface HJV—Approximately 5×10^5 intact HEK293 cells transiently transfected with HJV or empty vector were suspended in 0.2 ml of Dulbecco's modified Eagle's medium and incubated in the presence or absence of PI-PLC (ProZyme, San Leandro, CA) at a concentration of 1 unit/ml for 2 h at 37 °C in 5% CO_2 incubator. Cells were separated from the supernatant by centrifugation at 500 × *g* for 5 min. Both cell lysates and supernatants were subjected to 8% SDS-PAGE, followed by immunodetection of HJV using rabbit anti-HJV antibody at 1:10,000 dilution as described under "Immunodetection on Western Blots."

Immunoprecipitation—Immunoprecipitation was performed as described previously (36, 37) with some modifications. Briefly, 50 μl of Pansorbin (Calbiochem) was first coated with antibody by incubation with 2 μl of either rabbit anti-HJV serum or 2 μg of rabbit anti-neogenin antibody in 50 μl of NET/Triton buffer (150 mM NaCl, 5 mM EDTA, and 10 mM Tris (pH 7.4) with 1% Triton X-100) for 50 min at 4 °C. After removing the unbound antibody by washing with NET/Triton buffer, pre-absorbed cell lysate as indicated below was added and incubated at 4 °C for 50 min, followed by washing twice with NET/Triton buffer. Samples were eluted in 100 μl of 2× Laemmli buffer (125 mM Tris-HCl (pH 6.8), 4% SDS, 20% glycerol, and 10% 2-mercaptoethanol) (38) and subjected to SDS-PAGE on 8% acrylamide gels under reducing conditions. Immunodetection was performed as described above, except that rabbit TrueBlot (catalog no. 18-8816, eBioscience) at 1:1000 dilution was used as the secondary antibody. This secondary antibody was used to immunodetect protein immunoprecipitated with rabbit antibodies. It does not recognize denatured IgG; and thus, no IgG bands were visible on the immunoblots.

Tf-^{55}Fe Uptake—Steady state levels of Tf-^{55}Fe uptake were measured as described previously with some modifications (37). Briefly, Myc-HJV HEK293 and control HEK293 cells were transiently transfected with full-length human neogenin cDNA as described above. One day after transfection, the medium was replaced with fresh complete medium (Dulbecco's modified Eagle's medium plus 10% fetal calf serum and 800 μg/ml G418) and 0.5 μM Tf-^{55}Fe. Cells were then incubated in an CO_2

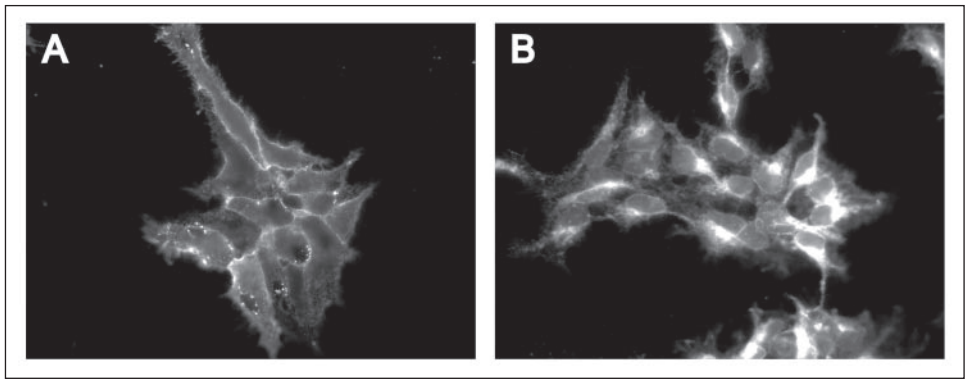

FIGURE 2. **HJV is found both on the cell surface and in internal compartments.** Cells stably expressing Myc-HJV were fixed and either left non-permeabilized (*A*) or permeabilized with 0.2% Triton X-100 (*B*). Cells were incubated with purified anti-Myc monoclonal antibody at 1:20 dilution for 1 h at room temperature, followed by incubation with Alexa 594-labeled donkey anti-mouse antibody at 1:500 dilution. Images were taken with a ×60 oil immersion lens. Experiments were repeated three times with consistent results. In all experiments, HEK293 cells stably transfected with the pcDNA3 empty vector served as a negative control. No staining was detected (data not shown).

incubator for ~24 h, followed by acid washing to remove surface-bound Tf-^{55}Fe. The amount of ^{55}Fe in cells is expressed as pmol of ^{55}Fe/mg of cellular protein/24 h. In a parallel experiment, the transfection efficiency of neogenin cDNA was evaluated by immunofluorescence analysis using rabbit anti-neogenin antibody. About 15% of the cells were strongly positive. Each set of experiments was conducted in quadruplicate.

Real-time PCR—Real-time PCR was performed as described previously (39, 40). RNA from Myc-HJV HEK293 and control HEK293 cells was isolated using the RNeasy RNA isolation kit (Qiagen Inc.). The message levels of glyceraldehyde-3-phosphate dehydrogenase (GAPDH), DMT1, FPN, ferritin light and heavy chains, TfR1, HJV, and neogenin were measured. The primer sequences for GAPDH, DMT1, FPN, TfR1, and ferritin light and heavy chains were the same as reported previously (40). The primers for HJV were 5′-gttcttgcattgcgcttcct-3′ (forward) and 5′-gctccttggacacggcat-3′ (reverse). The primers for neogenin were 5′-acagcctccatcgggactcta-3′ (forward) and 5′-gctactctcggagtcttccaaca-3′ (reverse). The results for each gene of interest are expressed as the amount relative to that of GAPDH in each cell line.

Neogenin Knockdown Using Small Interfering RNA (siRNA)—siRNA for neogenin (human NEO1) was purchased from Dharmacon RNA Technologies to knock down the endogenous neogenin in HEK293 cells. siRNA was transfected into the cells using Oligofectamine (Invitrogen) at a concentration of 100 nM for 48 h following the manufacturer's instruction. Cells were treated with 5 μM Tf for 24 h prior to harvesting to enhance the ferritin signal. The protein levels of neogenin, ferritin, and HJV were detected by Western blotting as described above under "Immunodetection on Western Blots."

RESULTS

HJV Is a Membrane-associated Protein—Immunofluorescence of non-permeabilized and permeabilized cells was used to determine the localization of HJV in cells. In the non-permeabilized cells, Myc-HJV was evenly distributed on the plasma membrane (Fig. 2*A*), indicating that Myc-HJV traffics to the cell surface and is a membrane-associated protein. In the Triton X-100-permeabilized cells, HJV was also found in perinuclear organelles within cells (Fig. 2*B*).

Characterization of HJV Processing in HEK293 Cells and sHJV—Full-length HJV cDNA encodes a 426-amino acid protein including an N-terminal signal peptide of 33 amino acids in length. Immunoblot analysis of Myc-HJV expressed in HEK293 cells using anti-HJV serum detected three bands migrating at ~50, 33, and 14 kDa (Fig. 3*A*) under denaturing and reducing conditions. Three bands were also detected in purified preparations of truncated sHJV (Fig. 3*A*). To characterize the origin of the bands, two additional antibodies were used. The anti-Myc antibody detected the 50- and 14-kDa bands, implying that the 14-kDa protein is a cleavage product containing the N terminus of HJV. When the same blot was reprobed with an antibody raised against a peptide corresponding to amino acids 321–335 of HJV (24), an additional band at 33 kDa was detected (Fig. 3*A*, *dotted arrow*). HJV contains three potential *N*-linked glycosylation sites and is predicted, based on a consensus sequence proximal to the transmembrane domain and the lack of a cytoplasmic domain, to be a glycosylphosphatidylinositol (GPI)-linked protein. Thus, the 50-kDa band is most likely the full-length protein; the 14-kDa band is the N-terminal portion with a single *N*-linked glycosylation site; and the 33-kDa band is the C-terminal portion of HJV with two *N*-linked glycosylation sites. The sHJV recombinant protein purified from the supernatant of Sf9 insect cells was also processed similarly (Fig. 3*A*).

In contrast to the multiple bands detected under reducing conditions, when the gels were run under nonreducing conditions, only a single band was apparent at 45 kDa in HEK293 cells expressing HJV and at ~40 kDa for sHJV (Fig. 3*B*). The mouse family of RGMs has 12 highly conserved Cys residues in their ectodomains. These Cys residues are also conserved in HJV. The single bands detected at 45 kDa under nonreducing conditions in Myc-HJV HEK293 cell extract and at ~40 kDa in sHJV are consistent with the joining of the cleaved protein fragments by disulfide bonds.

Proteolytic Processing of HJV—Examination of the partial von Willebrand factor D domains of HJV and the RGMs revealed sequence similarity to a group of proteins that appear to undergo autocatalytic cleavage (41). Specifically, the sequence Gly-Asp-Pro-His (present in HJV and the RGMs) is known to be cleaved in the human MUC2 mucin, the sialomucin complex, and heavy chain 3 of the pre-α-inhibitor (41). Asp–Pro bonds are well known to be labile under strongly acidic (but non-physiological) conditions. Presumably, the Gly-Asp-Pro-His sequences in these proteins are naturally cleaved under mildly acidic conditions due to a specific conformation and/or general acid catalysis. mRGMa, mRGMb, and mRGMc and chicken RGM have been observed to be cleaved at identical sites (24), but the similarity to other proteins with a Gly-Asp-Pro-His motif has not been noted previously.

In the case of mucin, cleavage was attenuated by neutralizing the pH within the lumen of the intracellular organelle by NH_4Cl (41). To determine whether the cleavage of HJV is inhibited at higher pH, Myc-HJV HEK293 cells were treated overnight with 25 mM NH_4Cl. Western blot analysis of HJV under reducing conditions showed that, in comparison with untreated cells, treatment with NH_4Cl significantly decreased the intensity of the 33-kDa band (Fig. 3*C*). These results demonstrate that cleavage was reduced by NH_4Cl treatment and, taking the size of the cleavage products into account, indirectly indicate that cleavage of the Asp–Pro bond is most likely responsible for generation of the 33- and 14-kDa peptides. Conversely, incubation of purified recombinant sHJV at pH 5.5 increased cleavage, further supporting the idea that HJV undergoes partial autocatalytic cleavage (Fig. 3*D*). When the three potential *N*-glycosylation sites are taken into account, the molecular masses of bands

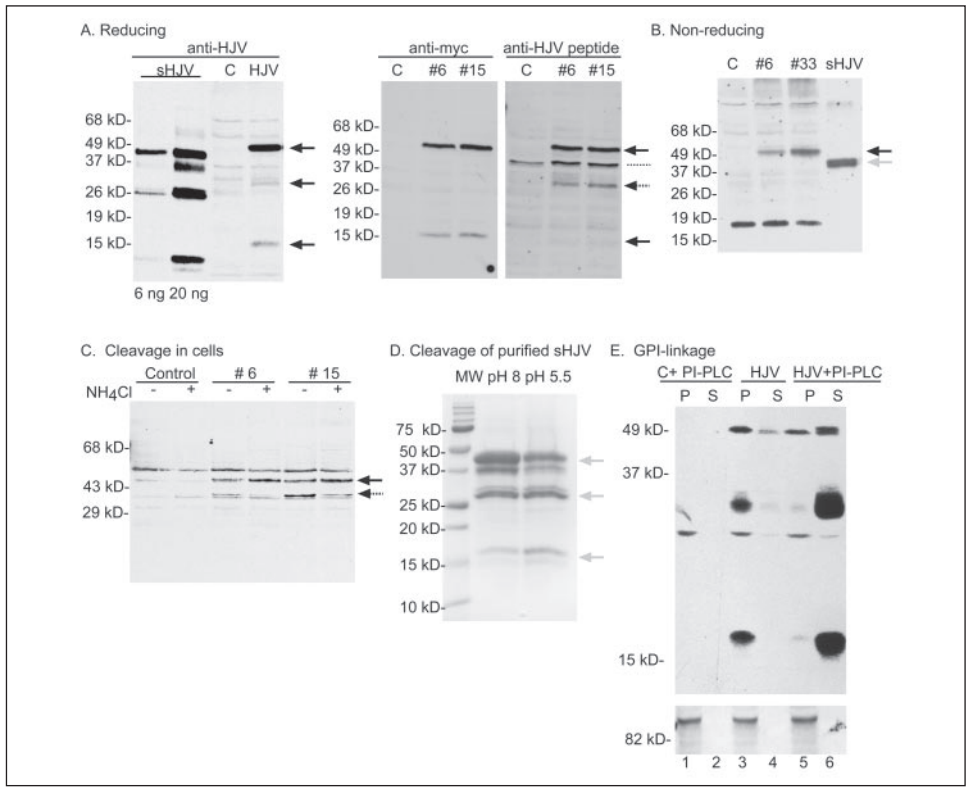

FIGURE 3. **HJV is extensively modified by cleavage, disulfide bond formation, and GPI addition.** *A*, sHJV and cell extracts from mock-transfected control cells (*C*) and Myc-HJV HEK293 cells (*HJV*) were subjected to Western blotting. Purified sHJV (6 and 20 ng) and cell extracts (50 μg) were subjected to SDS-PAGE on 12% polyacrylamide gels under reducing conditions before transfer to nitrocellulose. Blots were probed with anti-HJV serum generated against purified sHJV. *Black arrows* indicate full-length HJV and processed forms in cell extracts. In the second set of experiments, the first blot was probed with anti-Myc monoclonal antibody and then reprobed with anti-HJV peptide antibody (raised against the C-terminal region of HJV). The three cleavage products (*black arrows*) were seen in HEK293 cells expressing full-length Myc-HJV, and the nonspecific band (*dotted line*) was seen in untransfected cells. *B*, Western blots of the same extracts in *A* were subjected to nonreducing SDS-PAGE, transferred to nitrocellulose, and probed with rabbit anti-HJV serum. *C*, cells expressing HJV were treated overnight with 25 mM NH_4Cl to increase the pH of the HJV-processing compartments before solubilization and then subjected to SDS-PAGE under reducing conditions and immunoblot analysis of the cleavage products of HJV. Cells transfected with empty vector were used as a control. Two clonal cell lines (clones 6 and 15) were tested. In all cases, the blots were probed with rabbit anti-HJV peptide antibody at 1:1000 dilution and horseradish peroxidase-conjugated goat anti-rabbit antibody at 1:5000 dilution and visualized by chemiluminescence. *D*, shown is the cleavage of purified sHJV. Purified sHJV (7 μg) was incubated in either pH 8 or 5.5 buffer for 6 h at 37 °C and subjected to SDS-PAGE under reducing conditions, and the gels were stained with Coomassie Blue to visualize the protein. *E*, shown are the phospholipase C cleavage of the GPI linkage and release of HJV from the cell membrane. Empty vector-transfected cells and HJV-transfected HEK293 cells were treated in the presence (*C+PI-PLP* and *HJV+PI-PLC*, respectively) or absence (*HJV*) of PI-PLC in Dulbecco's modified Eagle's medium (1 unit/ml) for 2 h at 37 °C in a CO_2 incubator, and the cells were pelleted by centrifugation at 500 × *g* for 5 min and separated from the supernatant (*S*). Cell lysates were prepared from the pellet (*P*) using NET/Triton buffer. Samples were subjected to SDS-12% PAGE under reducing conditions before transfer to nitrocellulose. The blot was cut at the 68-kDa prestained molecular mass marker. The blot was probed with anti-HJV serum at 1:10,000 dilution (*upper panel*) and with sheep anti-TfR antibody at 1:10,000 dilution (*lower panel*). All experiments were repeated at least twice with consistent results.

detected by Western blotting match the predicted molecular masses of fragments generated by cleavage of the Asp–Pro bond.

HJV Is a GPI-linked Membrane Protein—A sequence proximal to the transmembrane domain and the lack of a cytoplasmic domain in HJV predict that HJV is a GPI-linked protein. To verify this, HJV-transfected HEK293 cells were treated with PI-PLC, an enzyme that specifically hydrolyzes the phosphodiester bond of phosphatidylinositol to release the GPI-linked proteins from membranes (42). Treatment of cells with PI-PLC led to the release of the majority of HJV into the medium (Fig. 3*E*, *lane 6*), in agreement with the prediction that it is a GPI-linked membrane protein. The HJV still remaining cell-associated after PI-PLC treatment is consistent with the results of immunofluorescence analysis and reflects an internal pool of HJV. Interestingly, a detectable amount of HJV was also found in the supernatant from the parallel control with no PI-PLC addition (Fig. 3*E*, *lane 4*), suggesting that HJV undergoes partial shedding in HEK293 cells. To rule out contaminating protease activities in the PI-PLC source, TfR, an integral membrane protein with a protease-sensitive cleavage site in the external domain, was used as a control. No TfR was detectable in the supernatant of PI-PLC-treated cells (Fig. 3*E*). These results indicate that HJV is a GPI-linked protein.

HJV Expression Increases Ferritin Levels in HJV-transfected HEK293 Cells—Because mutations in HJV cause Type 2A HH, we next examined the effect of HJV expression on iron homeostasis in Myc-HJV HEK293 cells. The levels of intracellular ferritin, an iron storage protein, were used as an indicator of cellular iron status. The synthesis of ferritin is controlled translationally by the binding of iron regulatory proteins to an iron-responsive element in the 5′-untranslated region of its mRNA (1). In general, increases in ferritin levels reflect increases in intracellular iron. Two different clones (clones 6 and 15) of cells stably expressing Myc-HJV (Fig. 4*A*) were tested for ferritin levels. Because the ferritin levels are normally low in this cell line, cells were treated either with physiological levels of human transferrin (5 μM holo-Tf) or with 20 μg/ml ferric ammonia citrate to increase the basal ferritin levels. Increases in ferritin levels upon HJV expression became apparent under these conditions (Fig. 4*B*). Tf-mediated iron uptake by the cells is through TfR-mediated endocytosis, whereas the acquisition of iron by the cells from ferric ammonia citrate is through an undefined pathway. The higher ferritin levels upon treatment of the cells with either form of iron suggest that HJV enhances iron accumulation or that it inhibits iron efflux from these cells.

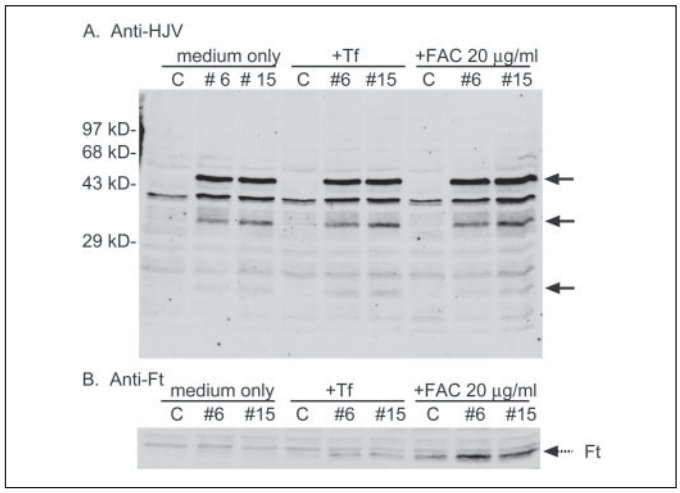

FIGURE 4. **Transfection of HJV into HEK293 cells results in increased levels of ferritin within the cells.** Two clonal cell lines (clones 6 and 15) transfected with Myc-HJV were tested for levels of HJV (*A*) and ferritin (*B*) by immunoblot analysis. *A*, cells expressing HJV (but not control empty vector-transfected cells (*C*)) showed full-length HJV and processed forms (*black arrows*). A nonspecific band at ~43 kDa was evident in both control and transfected cells. The blot was first probed with anti-Myc monoclonal antibody and then reprobed with anti-HJV peptide antibody (raised against the C-terminal region of HJV). *B*, ferritin levels were determined in cells grown overnight in medium alone or supplemented with human Tf (5 μM) or with ferric ammonium citrate (*FAC*; 20 μg/ml). Blots were probed sequentially with sheep anti-human ferritin (*Ft*) antibody at 1:1000 dilution for 2 h at room temperature and then with horseradish peroxidase-conjugated goat anti-sheep IgG (Chemicon Australia Pty. Ltd.) at 1:10,000 dilution for 1 h and visualized by chemiluminescence. Experiments were repeated three times with consistent results.

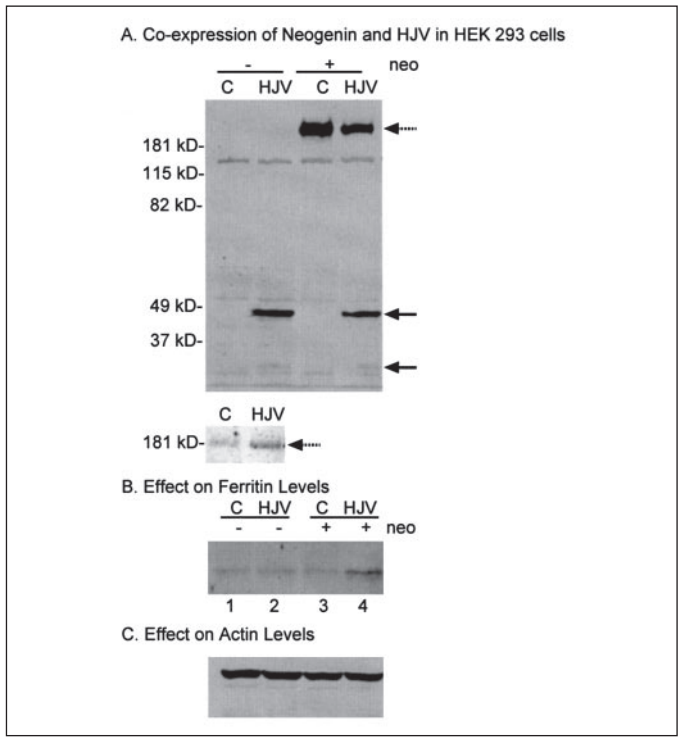

FIGURE 5. **Coexpression of neogenin and HJV in HEK293 cells results in increased ferritin levels compared with expression of HJV alone.** *A*, cells expressing HJV or control cells not expressing HJV (*C*) were transiently transfected with a plasmid coding for human neogenin. After 48 h, cells were lysed, and extracts (50 μg of cell lysate) were subjected to SDS-PAGE under reducing conditions, transferred to nitrocellulose, and probed with anti-HJV antibody (*solid arrows*) and anti-neogenin antibody (*dotted arrows*) at 1:500 dilution. The *lower panel* shows a longer exposure of the neogenin levels in control cells and HJV-expressing cells. *B* and *C*, duplicate gels were probed overnight at 4 °C with sheep anti-human ferritin antibody at 1:1000 dilution or with mouse anti-β-actin monoclonal antibody at 1:10,000 dilution as a loading control, respectively. Experiments were repeated four times with consistent results (see the first supplemental figure for another image).

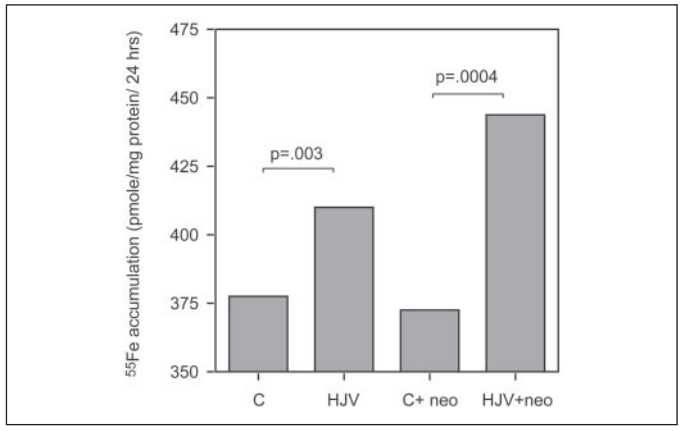

FIGURE 6. **^{55}Fe accumulation in HEK293 cells.** Empty vector-transfected control cells (*C*), Myc-HJV HEK293 cells (*HJV*), cells transiently transfected with neogenin (*C+neo*), and Myc-HJV HEK293 cells transiently transfected with neogenin (*HJV+neo*) were incubated for 24 h with 0.5 μM Tf-^{55}Fe in complete medium in quadruplicate. *p* values were calculated using Student's two-tailed *t* test. The experiment was repeated with similar results (see the second supplemental figure).

Neogenin Expression in Myc-HJV HEK293 Cells Further Enhances Ferritin Levels—To examine whether neogenin is involved in the HJV-mediated iron accumulation in HEK293 cells, neogenin was transiently transfected into both Myc-HJV HEK293 and control HEK293 cells with no Tf or ferric ammonia citrate supplementation of the medium as extra iron source. Immunofluorescence analysis of transfected cells using anti-neogenin antibody revealed that the transfection efficiency was ~15% (data not shown). The ferritin levels in these cell lysates were analyzed by Western blot analysis and compared with the HJV and neogenin levels (Fig. 5*B*). Equal protein loading was verified by β-actin detection. Expression of neogenin alone had no effect on ferritin levels, but expression of both HJV and neogenin together increased ferritin levels (Fig. 5*B*, *lanes 3* and *4 versus lanes 1* and *2*), which was detectable even without pretreating cells with iron. Interestingly, Western blot analysis of neogenin indicated that HEK293 cells endogenously express neogenin and that the levels of endogenously expressed neogenin increased when HJV was expressed (Fig. 5*A*, *lower panel*). The fact that HEK293 cells express low levels of neogenin explains the increases in iron accumulation that were observed in cells expressing HJV alone (Fig. 4*B*).

Expression of HJV and Neogenin in HEK293 Cells Increases ^{55}Fe Accumulation—To verify that ferritin levels reflect intracellular iron levels, we also measured the accumulation of ^{55}Fe by overnight incubation of cells with Tf-^{55}Fe. A modest but significant increase in iron accumulation (8.9%) was detected in HJV-expressing cells compared with control cells. When neogenin was transiently cotransfected into HJV-transfected HEK293 cells, an even greater increase in iron accumulation was observed (18.65% compared with control cells) (Fig. 6). In agreement with the anti-ferritin Western blot results, expression of neogenin alone did not show any effect on iron accumulation. These results again support the involvement of the HJV-neogenin complex in iron accumulation in HEK293 cells.

HJV Interacts with Neogenin—To explore the mechanism by which HJV increases iron loading of HEK293 cells, we first examined whether it interacts with TfR1 by co-immunoprecipitation studies using either anti-TfR1 or anti-HJV antibody. No complex of HJV with TfR1 could be detected (data not shown). HJV and its ortholog, mRGMc, are closely related to RGMa, which has been shown to bind to neogenin (22–24, 27, 28). To examine whether HJV also interacts with neogenin, three strategies were used. In the first set of experiments, we tested whether HJV

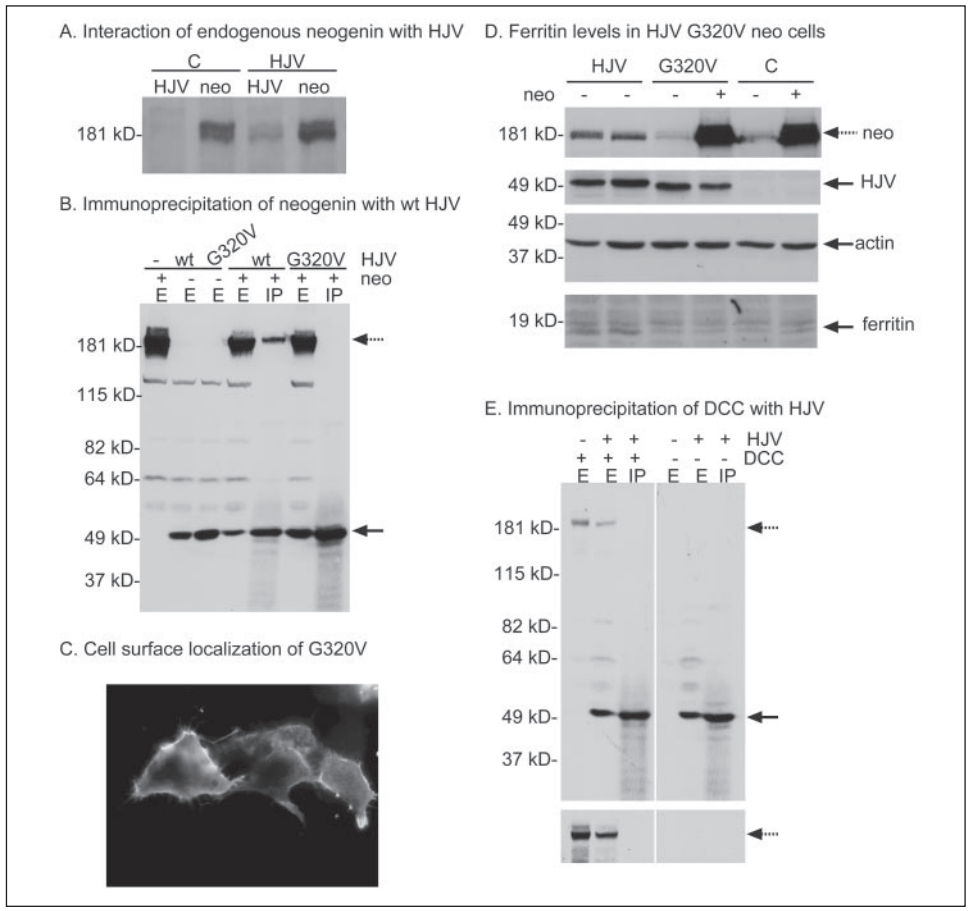

FIGURE 7. **Co-immunoprecipitation of neogenin with HJV.** *A*, Myc-HJV coprecipitated with endogenous neogenin in HEK293 cells. Lysates (~150 μg of protein) from Myc-HJV HEK293 cells (*HJV*) and control HEK293 cells (*C*) were immunoprecipitated using either rabbit anti-HJV serum (*HJV*) or rabbit anti-neogenin antibody (*neo*). Immunoprecipitates were subjected to SDS-PAGE under reducing conditions, transferred to nitrocellulose, and probed with anti-neogenin antibody. *B*, extracts from control HEK293 cells (*C*) or HEK293 cells transiently expressing either wild-type HJV (*wt*) or HJV G320V (*G320V*) were mixed with extracts from HEK293 cells transiently transfected with neogenin (*wt*+*neo* and *G320V*+*neo*) at equal amounts of protein. The mixed extracts (120 μg of protein) were immunoprecipitated with anti-HJV serum. The extracts (*E*) and immunoprecipitates (*IP*) were subjected to SDS-PAGE under reducing conditions, transferred to nitrocellulose, and probed with anti-HJV antibody to detect HJV (*solid arrow*). Anti-neogenin antibody was used to detect neogenin in cell extracts and immunoprecipitates (*dotted arrow*). *C*, cell-surface HJV G320V in stably transfected HEK293 cells under non-permeabilized conditions was visualized by immunofluorescence. Cells were fixed and incubated with rabbit anti-HJV serum at 1:400 dilution for 1 h at room temperature, followed by incubation with Alexa 594-labeled goat anti-rabbit antibody at 1:500 dilution. Images were taken using a ×60 oil immersion lens. *D*, the coexpression of neogenin and HJV G320V in HEK293 cells did not alter ferritin levels. Cells expressing HJV G320V (*G320V*) or control cells not expressing HJV (*C*) were transiently transfected with a plasmid coding for human neogenin. After 48 h, cells were lysed. Extracts (50 μg of protein) were subjected to SDS-PAGE under reducing conditions; transferred to nitrocellulose; and probed with anti-neogenin antibody at 1:500 dilution (*dotted arrow*) and anti-HJV, anti-β-actin, and anti-ferritin antibodies at 1:1000 dilution (*solid arrows*). The cell lysate from HJV-transfected HEK293 cells was also included as a control. *E*, extracts from HT29 cells stably transfected with DCC (*E*+*DCC*) were mixed with extracts from HEK293 cells transiently transfected with HJV (*E*+*HJV*) and immunoprecipitated with anti-HJV serum. The extracts (*E*) and immunoprecipitates (*IP*) were subjected to SDS-PAGE under reducing conditions, transferred to nitrocellulose, and probed with anti-HJV antibody to detect HJV (*solid arrow*). Anti-DCC antibody was used to detect DCC in cell extracts and immunoprecipitates (*dotted arrow*). The *lower panel* is a longer exposure of the *upper panel* showing no detectable DCC coprecipitating with HJV. The bands on the immunoblot were visualized with a horseradish peroxidase-conjugated anti-rabbit antibody that does not recognize the denatured heavy and light chains of rabbit IgG (eBioscience), followed by chemiluminescence. All experiments were repeated at least twice with consistent results.

interacts with endogenous neogenin in HEK293 cells using polyclonal antiserum to HJV. Immunoblot analysis indicated that endogenous neogenin co-immunoprecipitated with HJV (Fig. 7*A*). In the second set of experiments, neogenin was transiently transfected into Myc-HJV HEK293 cells, followed by immunoprecipitation using rabbit anti-HJV antibody. Neogenin co-immunoprecipitated with Myc-HJV, indicating that the Myc epitope did not interfere with the interaction (data not shown). In the third set of experiments, plasmids encoding neogenin and untagged HJV were transfected into separate batches of HEK293 cells. The solubilized cell lysates from the two populations were mixed and incubated for 1 h at 4 °C, followed by immunoprecipitation using anti-HJV antibody. In agreement with the finding in cells coexpressing Myc-HJV and neogenin, the antibody to HJV co-immunoprecipitated both HJV and neogenin (Fig. 7*B*), indicating that the two proteins bind to each other in solubilized extracts. These results demonstrate that both untagged HJV and Myc-HJV behave similarly. Thus, the HJV-neogenin complex has a high enough affinity to survive the rigors of immunoprecipitation.

HJV G320V Does Not Interact with Neogenin—To further characterize the interaction between HJV and neogenin, we examined the effect of the HJV G320V mutation, the most common mutation in Type 2A HH patients (6), by co-immunoprecipitation studies. It did not bind to neogenin in co-immunoprecipitation studies (Fig. 7*B*), even though HJV G320V appeared to be properly glycosylated and transported to the cell surface (Fig. 7*C*). Because HJV G230V did not bind neogenin, it failed to stabilize endogenously expressed neogenin and to increase ferritin levels (Fig. 7*D*). These results provide further support for the importance of the HJV/neogenin interaction in Type 2A HH.

HJV Does Not Interact with the Closely Related DCC—We also tested whether HJV interacts with DCC, a membrane protein closely related to neogenin (29–31), by mixing the cell lysate from HEK293 cells transiently transfected with HJV with the lysate from HT29 cells stably

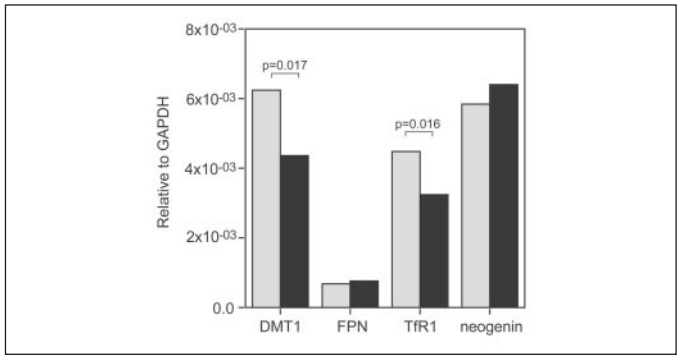

FIGURE 8. **Relative mRNA levels of iron-related proteins.** Quantitative reverse transcription-PCR was used to measure relative levels of the mRNAs of interest in mock-transfected control HEK293 cells (*gray bars*) and Myc-HJV HEK293 cells (*black bars*). All data were derived from three sets of cDNA preparations and were normalized to an internal standard (GAPDH). All mRNA levels are expressed as a -fold change relative to GAPDH. *p* values were calculated using Student's two-tailed *t* test (*HJV* mRNA levels: control HEK293 cells, 0.000049 ± 0.000024; Myc-HJV HEK293 cells, 0.617928 ± 0.041329).

expressing DCC. Immunoprecipitation studies using anti-HJV antiserum failed to pull down detectable DCC (Fig. 7*E*), despite the fact that both neogenin and DCC share nearly 50% amino acid identity (30). These results suggest that the interaction between HJV and neogenin is specific.

HJV Expression Decreases DMT1 and TfR1 mRNA Levels—To gain insight into how HJV interferes with iron homeostasis through binding to neogenin in HEK293 cells, we measured the mRNA levels of iron metabolism-related genes, including DMT1, *FPN*, TfR1, ferritin light and heavy chains, *HJV*, and neogenin, by quantitative real-time reverse transcription-PCR. The mRNA levels of *DMT1* and TfR1 in HJV-transfected HEK293 cells were significantly decreased by ~30 and 27%, respectively, in comparison with control HEK293 cells. As expression of these proteins is lowered under conditions of high cellular iron (1), these results are consistent with the ferritin blot results demonstrating that HJV expression results in higher iron levels. No significant changes in either ferritin light or heavy chain mRNA were detected (data not shown), consistent with the iron-mediated translational control of ferritin levels. Interestingly, the levels of endogenous neogenin mRNA were comparable with those of *DMT1* mRNA and did not increase upon HJV expression. Because we observed increased protein levels of neogenin in HJV-expressing cells, HJV could either stabilize the neogenin protein or increase translation of its message. To determine whether the HJV/neogenin interaction might affect iron efflux, we checked whether FPN, an iron exporter, is expressed in HEK293 cells. Detectable levels of *FPN* mRNA in HEK293 cells were measured (Fig. 8); thus, the ^{55}Fe accumulation detected in HJV-neogenin-transfected cells could be due to either increased iron uptake or decreased iron efflux.

DISCUSSION

Just over 1 year ago, mutations in *HJV* were identified as the causative factor in Type 2 HH (6). This finding was supported by subsequent studies by several other groups showing numerous additional mutations of *HJV* in JH patients (11–16). In this study, we characterized the processing of HJV expressed in HEK293 cells and identified a binding interaction with neogenin that increases iron accumulation in HEK293 cells.

HJV is a member of the RGM family of proteins (24). Included in this family is chicken RGM, a homolog of the GPI-linked protein mRGMa (24, 26). We found that HJV is sensitive to PI-PLC digestion, indicating that it, too, is a GPI-anchored protein. GPI-anchored proteins can be shed from the membrane in a soluble form by membrane secretase-like proteolytic cleavage and/or phospholipase cleavage of the GPI anchor moiety (43–45). The soluble form can then enter the circulation and bind distant receptors. mRGMc, the ortholog of HJV, is efficiently shed from transiently transfected COS-7 cells (24), raising the possibility that the release of HJV from a tissue such as muscle might allow it to interact with a receptor on another tissue such as the liver. We failed to detect any soluble form of HJV in the conditioned medium from HJV-transfected HEK293 cells by Western blotting (data not shown). This might be due to a lack of sensitivity of our anti-HJV antibody or the lack of appropriate enzymes for cleavage in HEK293 cells. HEK293 cells are derived from the kidney; the kidney does not show HJV expression by Northern blot analysis (6), and we did not detect any endogenous levels of HJV.

In addition to the GPI linkage, HJV undergoes other post-translational modifications. HJV and the mRGMs possess a Gly-Asp-Pro-His sequence (6, 24). Previous studies showed that the Asp–Pro bond in this sequence undergoes partial autocatalytic cleavage at pH <6.0 in the human MUC2 mucin, the sialomucin complex, and heavy chain 3 of the pre-α-inhibitor (41). RGMa is also cleaved at this Asp–Pro bond (24). Three different antibodies that detect distinct epitopes were used to characterize HJV processing within HEK293 cells. Our results show that HJV undergoes a similar pattern of processing consistent with cleavage being at this Asp–Pro bond. A single band detected on nonreducing gels indicates that the cleaved peptides are linked by disulfide bonds. In addition, this pattern of cleavage was observed in sHJV generated from both Sf9 cells and HEK293 cells as well (data not shown). In agreement with these findings, the Asp–Pro bond in chicken RGMa was also found to be cleaved in transfected HEK293 cells, although the cleavage appeared to be more efficient (26). Notably, the cleavage of HJV was observed in mouse tissues by Western blot analysis using anti-HJV peptide antibody, which revealed 26- and 30-kDa bands (46). The lack of full-length HJV in mouse tissues (46) implies that it has been either shed or completely processed at this Asp–Pro bond. The more complete cleavage detected in mouse tissues compared with our findings might be due to tissue-specific processing.

In this study, we found that the function of HJV in the regulation of iron accumulation depends on its interaction with neogenin in HEK293 cells. Expression of HJV resulted in a modest increase in ferritin levels, and expression of neogenin enhanced this effect. HJV expression increased iron accumulation from both Tf and non-Tf iron sources, whereas neogenin expression alone had no significant effect in HEK293 cells. These latter results suggest that the HJV-neogenin complex is necessary for iron accumulation within cells. We attempted to knock down the endogenous neogenin using siRNA to further verify that neogenin is responsible for the HJV-induced changes in iron homeostasis. Treatment of cells with siRNA resulted in only an ~40% reduction in neogenin protein levels, still well above the levels in control HEK293 cells (data not shown). This might be due to the stabilization of neogenin protein by HJV.

The proposal that HJV-induced changes in iron homeostasis require interaction with neogenin is supported by the observation that the HJV G320V mutation, the most common mutation in Type 2A HH (6, 14), neither interacted with neogenin nor altered intracellular iron levels. Notably, expression of HJV overlapped with that of neogenin in muscles and liver, but not with expression of two other RGM family members, RGMa and RGMb (22–24,30). Although neogenin is also a receptor for netrins, their interactions are involved mainly in neural development (47–49). For example, in netrin-1-deficient mice, defects include the aberrant development of hippocampal circuits and altered neural activity, with no apparent abnormality in iron homeostasis reported (50). This implies that netrins are not involved in the regulation of iron metabolism. Human neogenin has two alternatively spliced forms

encoding proteins of 1461 and 1408 amino acid, respectively, with the deletion of 53 amino acids in the cytoplasmic domain of the latter including the loss of three potential phosphorylation sites. The common extracellular portion consists of four immunoglobulin-like and six fibronectin type III-like domains (30). We speculate that each ligand binds to a preferential isoform of neogenin, a distinct domain in neogenin, or a combination of both to trigger the corresponding signal transduction pathway in specific target cells resulting in different consequences. More specifically, binding of HJV to neogenin in muscles and liver would be assumed to activate the signal transduction pathway(s) involved in the regulation of iron homeostasis. In addition, failure of the HJV G320V mutant to interact with neogenin and to alter cellular iron levels also implies that Type 2A JH is due to the loss of HJV function.

The observation that HJV interacts with neogenin opens up the possibility that HJV stimulates intracellular signaling events. Neogenin is a transmembrane protein widely expressed in different adult tissues (31). It is the receptor for a variety of ligands such as RGMa and netrins (27, 28, 48). Neogenin binding to RGMa has two important functions: regulation of neuronal survival and guidance of axon growth during development (27, 28, 51). In the neural tube, RGMa functions as a cell survival factor by repressing the pro-apoptotic activity of neogenin (28). The binding of netrins to neogenin is involved in neural development, although studies have also indicate a role in epithelial morphogenesis and myotube formation (47–49). Netrins are a small family of secreted laminin-like proteins originally identified as neuronal guidance cues. Netrins have at least six different receptors. In addition to neogenin, netrins also bind to DCC and four UNC5 proteins (UNC5A–D in the human and UNC5H1–4 in the mouse) (47). In neuronal development, netrins can either attract or repel axonal projections depending upon the receptors with which they interact on the neuronal growth cones (47). In addition, the interaction of netrin-1 with its receptors (DCC and the UNC5 molecules) is implicated in the regulation of apoptosis, implying an important role in tumorigenesis (52). All these processes tend to be accomplished through signal transduction pathways (47, 49, 51). The above findings indicate that neogenin has multiple ligands and exerts different functions based upon its spatial and temporal association with its ligand. This notion is supported by studies of neogenin knockout in early zebrafish embryos indicating a role for neogenin in determining cell polarity or directionality of migration in both neuroectodermal and mesodermal cells (32). The fact that neogenin couples with different signaling complexes in a cell type- and ligand-specific manner raises the possibility that the HJV-neogenin complex could result in a signaling cascade in the liver, ultimately affecting hepcidin production.

Type 2A HH patients with mutations in HJV have decreased levels of hepcidin, indicating the involvement of HJV in the regulation of hepcidin synthesis (6). *HJV* mRNA levels are highest in skeletal muscle, followed by liver and heart (6), whereas hepcidin is expressed predominantly in hepatocytes (17, 18, 39), with little or no expression in skeletal muscle.[3] Thus, HJV and hepcidin have only a limited overlap in tissue expression. The liver is a critical organ in the regulation of body iron homeostasis, important for iron storage and the synthesis of transferrin, ceruloplasmin, and hepcidin. Skeletal and cardiac muscles require iron for incorporation into the heme of myoglobin (53). Based on the need for iron in muscles, the abundance of HJV in muscle, the lack of regulation of HJV at the mRNA levels by iron loading in mice (21), and our present results, we propose a model by which HJV and neogenin interact to regulate iron homeostasis. In skeletal muscle cells, HJV-neogenin complex formation regulates intracellular iron levels for incorporation into the heme of myoglobin. HJV in skeletal muscle is shed and enters the circulation as a soluble form of HJV. The amount of shedding could be regulated by iron supply in muscle, oxygen tension in the circulation, or other factors. The binding of HJV to neogenin and perhaps other coreceptors on hepatocytes up-regulates hepcidin mRNA through as yet unidentified signaling pathways. Lack of functional HJV would result in low levels of hepcidin and increased iron uptake by the intestines. Full understanding of this pathway is the next challenge.

Acknowledgments—We thank Dr. Silvia Arber for rabbit anti-HJV peptide antibody, Dr. Jan Christian for mouse anti-Myc monoclonal antibody, Dr. Eric R. Fearon for human neogenin cDNA, Dr. Anna Velcich for HT29-DCC11 and HT29-neo cells, and members of the Enns laboratory for critical reading of the manuscript.

[3] A.-S. Zhang and C. A. Enns, unpublished data.

REFERENCES

1. Hentze, M. W., Muckenthaler, M. U., and Andrews, N. C. (2004) *Cell* **117,** 285–297
2. Pietrangelo, A. (2004) *N. Engl. J. Med.* **350,** 2383–2397
3. Feder, J. N., Gnirke, A., Thomas, W., Tsuchihashi, Z., Ruddy, D. A., Basava, A., Dormishian, F., Domingo, R. J., Ellis, M. C., Fullan, A., Hinton, L. M., Jones, N. L., Kimmel, B. E., Kronmal, G. S., Lauer, P., Lee, V. K., Loeb, D. B., Mapa, F. A., McClelland, E., Meyer, N. C., Mintier, G. A., Moeller, N., Moore, T., Morikang, E., Prasss, C. E., Quintana, L., Starnes, S. M., Schatzman, R. C., Brunke, K. J., Drayna, D. T., Risch, N. J., Bacon, B. R., and Wolff, R. K. (1996) *Nat. Genet.* **13,** 399–408
4. De Gobbi, M., Roetto, A., Piperno, A., Mariani, R., Alberti, F., Papanikolaou, G., Politou, M., Lockitch, G., Girelli, D., Fargion, S., Cox, T. M., Gasparini, P., Cazzola, M., and Camaschella, C. (2002) *Br. J. Haematol.* **117,** 973–979
5. Camaschella, C., Roetto, A., and De Gobbi, M. (2002) *Semin. Hematol.* **39,** 242–248
6. Papanikolaou, G., Samuels, M. E., Ludwig, E. H., MacDonald, M. L., Franchini, P. L., Dube, M. P., Andres, L., MacFarlane, J., Sakellaropoulos, N., Politou, M., Nemeth, E., Thompson, J., Risler, J. K., Zaborowska, C., Babakaiff, R., Radomski, C. C., Pape, T. D., Davidas, O., Christakis, J., Brissot, P., Lockitch, G., Ganz, T., Hayden, M. R., and Goldberg, Y. P. (2004) *Nat. Genet.* **36,** 77–82
7. Roetto, A., Totaro, A., Cazzola, M., Cicilano, M., Bosio, S., D'Ascola, G., Carella, M., Zelante, L., Kelly, A. L., Cox, T. M., Gasparini, P., and Camaschella, C. (1999) *Am. J. Hum. Genet.* **64,** 1388–1393
8. Papanikolaou, G., Politou, M., Roetto, A., Bosio, S., Sakelaropoulos, N., Camaschella, C., and Loukopoulos, D. (2001) *Blood Cells Mol. Dis.* **27,** 744–749
9. Papanikolaou, G., Papaioannou, M., Politou, M., Vavatsi, N., Kioumi, A., Tsiatsiou, P., Marinaki, P., Loukopoulos, D., and Christakis, J. I. (2002) *Blood Cells Mol. Dis.* **29,** 168–173
10. Rivard, S. R., Lanzara, C., Grimard, D., Carella, M., Simard, H., Ficarella, R., Simard, R., D'Adamo, A. P., Ferec, C., Camaschella, C., Mura, C., Roetto, A., De Braekeleer, M., Bechner, L., and Gasparini, P. (2003) *Eur. J. Hum. Genet.* **11,** 585–589
11. Huang, F. W., Rubio-Aliaga, I., Kushner, J. P., Andrews, N. C., and Fleming, M. D. (2004) *Blood* **104,** 2176–2177
12. Lanzara, C., Roetto, A., Daraio, F., Rivard, S., Ficarella, R., Simard, H., Cox, T. M., Cazzola, M., Piperno, A., Gimenez-Roqueplo, A. P., Grammatico, P., Volinia, S., Gasparini, P., and Camaschella, C. (2004) *Blood* **103,** 4317–4321
13. Lee, P. L., Beutler, E., Rao, S. V., and Barton, J. C. (2004) *Blood* **103,** 4669–4671
14. Gehrke, S., Pietrangelo, A., Kascak, M., Braner, A., Eisold, M., Kulaksiz, H., Herrmann, T., Hebling, U., Bents, K., Gugler, R., and Stremmel, W. (2005) *Clin. Genet.* **67,** 425–428
15. Barton, J. C., Rivers, C. A., Niyongere, S., Bohannon, S. B., and Acton, R. T. (2004) *BMC Medical Genetics* http://www.biomedcentral.com/1471-2350/5/29
16. Janosi, A., Andrikovics, H., Vas, K., Bors, A., Hubay, M., Sapi, Z., and Tordai, A. (2005) *Blood* **105,** 432
17. Krause, A., Neitz, S., Magert, H. J., Schulz, A., Forssmann, W. G., Schulz-Knappe, P., and Adermann, K. (2000) *FEBS Lett.* **480,** 147–150
18. Park, C. H., Valore, E. V., Waring, A. J., and Ganz, T. (2001) *J. Biol. Chem.* **276,** 7806–7810
19. Nemeth, E., Tuttle, M. S., Powelson, J., Vaughn, M. B., Donovan, A., Ward, D. M., Ganz, T., and Kaplan, J. (2004) *Science* **306,** 2090–2093
20. Nicolas, G., Chauvet, C., Viatte, L., Danan, J. L., Bigard, X., Devaux, I., Beaumont, C., Kahn, A., and Vaulont, S. (2002) *J. Clin. Investig.* **110,** 1037–1044
21. Krijt, J., Vokurka, M., Chang, K. T., and Necas, E. (2004) *Blood* **104,** 4308–4310
22. Schmidtmer, J., and Engelkamp, D. (2004) *Gene Expr. Patterns* **4,** 105–110
23. Oldekamp, J., Kramer, N., Alvarez-Bolado, G., and Skutella, T. (2004) *Gene Expr. Patterns* **4,** 283–288
24. Niederkofler, V., Salie, R., Sigrist, M., and Arber, S. (2004) *J. Neurosci.* **24,** 808–818
25. Brinks, H., Conrad, S., Vogt, J., Oldekamp, J., Sierra, A., Deitinghoff, L., Bechmann, I.,

Alvarez-Bolado, G., Heimrich, B., Monnier, P. P., Mueller, B. K., and Skutella, T. (2004) *J. Neurosci.* **24,** 3862–3869
26. Monnier, P. P., Sierra, A., Macchi, P., Deitinghoff, L., Andersen, J. S., Mann, M., Flad, M., Hornberger, M. R., Stahl, B., Bonhoeffer, F., and Mueller, B. K. (2002) *Nature* **419,** 392–395
27. Rajagopalan, S., Deitinghoff, L., Davis, D., Conrad, S., Skutella, T., Chedotal, A., Mueller, B. K., and Strittmatter, S. M. (2004) *Nat. Cell Biol.* **6,** 756–762
28. Matsunaga, E., Tauszig-Delamasure, S., Monnier, P. P., Mueller, B. K., Strittmatter, S. M., Mehlen, P., and Chedotal, A. (2004) *Nat. Cell Biol.* **6,** 749–755
29. Vielmetter, J., Kayyem, J. F., Roman, J. M., and Dreyer, W. J. (1994) *J. Cell Biol.* **127,** 2009–2020
30. Meyerhardt, J. A., Look, A. T., Bigner, S. H., and Fearon, E. R. (1997) *Oncogene* **14,** 1129–1136
31. Keeling, S. L., Gad, J. M., and Cooper, H. M. (1997) *Oncogene* **15,** 691–700
32. Mawdsley, D. J., Cooper, H. M., Hogan, B. M., Cody, S. H., Lieschke, G. J., and Heath, J. K. (2004) *Dev. Biol.* **269,** 302–315
33. Velcich, A., Corner, G., Palumbo, L., and Augenlicht, L. (1999) *Oncogene* **18,** 2599–2606
34. Lebron, J. A., Bennett, M. J., Vaughn, D. E., Chirino, A. J., Snow, P. M., Mintier, G. A., Feder, J. N., and Bjorkman, P. J. (1998) *Cell* **93,** 111–123
35. Carlson, H., Zhang, A. S., Fleming, W. H., and Enns, C. A. (2005) *Blood* **105,** 2564–2570
36. Gross, C. N., Irrinki, A., Feder, J. N., and Enns, C. A. (1998) *J. Biol. Chem.* **273,** 22068–22074
37. Zhang, A. S., Davies, P. S., Carlson, H. L., and Enns, C. A. (2003) *Proc. Natl. Acad. Sci. U. S. A.* **100,** 9500–9505
38. Laemmli, U. K. (1970) *Nature* **227,** 680–685
39. Zhang, A. S., Xiong, S., Tsukamoto, H., and Enns, C. A. (2004) *Blood* **103,** 1509–1514
40. Davies, P. S., and Enns, C. A. (2004) *J. Biol. Chem.* **279,** 25085–25092
41. Lidell, M. E., Johansson, M. E., and Hansson, G. C. (2003) *J. Biol. Chem.* **278,** 13944–13951
42. Menon, A. K. (1994) *Methods Enzymol.* **230,** 418–442
43. Parkin, E. T., Watt, N. T., Turner, A. J., and Hooper, N. M. (2004) *J. Biol. Chem.* **279,** 11170–11178
44. Levine, S. J. (2004) *J. Immunol.* **173,** 5343–5348
45. Hooper, N. M., Karran, E. H., and Turner, A. J. (1997) *Biochem. J.* **321,** 265–279
46. Rodriguez Martinez, A., Niemela, O., and Parkkila, S. (2004) *Haematologica* **89,** 1441–1445
47. Nikolopoulos, S., and Giancotti, F. (2005) *Cell Cycle* **4,** 131–135
48. Srinivasan, K., Strickland, P., Valdes, A., Shin, G. C., and Hinck, L. (2003) *Dev. Cell* **4,** 371–382
49. Kang, J. S., Yi, M. J., Zhang, W., Feinleib, J. L., Cole, F., and Krauss, R. S. (2004) *J. Cell Biol.* **167,** 493–504
50. Barallobre, M. J., Del Rio, J. A., Alcantara, S., Borrell, V., Aguado, F., Ruiz, M., Carmona, M. A., Martin, M., Fabre, M., Yuste, R., Tessier-Lavigne, M., and Soriano, E. (2000) *Development* (*Camb.*) **127,** 4797–4810
51. Matsunaga, E., and Chedotal, A. (2004) *Dev. Growth Differ.* **46,** 481–486
52. Arakawa, H. (2004) *Nat. Rev. Cancer* **4,** 978–987
53. Ordway, G. A., and Garry, D. J. (2004) *J. Exp. Biol.* **207,** 3441–3446